

# U-Pb and U-Th-Pb Geochronology

## 1. Isotopes

Elements are defined by the number of protons in the nucleus, but some elements can have multiple different numbers of neutrons. For example, oxygen always has eight protons, but there are three isotopes of oxygen:  $^{16}\text{O}$ ,  $^{17}\text{O}$ , and  $^{18}\text{O}$ , which have 8, 9, and 10 neutrons, respectively.

Stable Isotope: an isotope that has a stable nucleus and will never undergo radioactive decay.

Radioactive Isotope: an isotope whose nucleus is energetically unstable and will eventually decay to a different element.

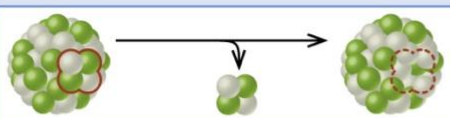
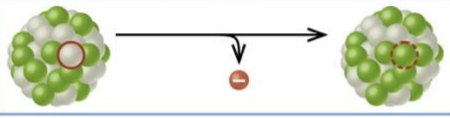
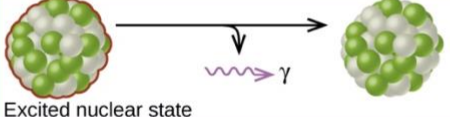
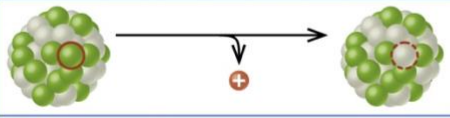
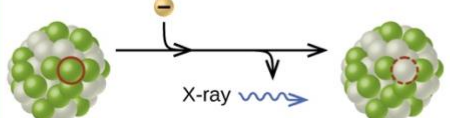
Some elements (like oxygen) only have stable isotopes; others may have one or more radioactive isotopes, and some elements have no stable isotopes. For example, potassium (K) has two stable isotopes ( $^{39}\text{K}$  and  $^{41}\text{K}$ ) and one radioactive isotope ( $^{40}\text{K}$ ). Uranium has no stable isotopes – all of its naturally-occurring isotopes are radioactive:  $^{233}\text{U}$ ,  $^{234}\text{U}$ ,  $^{235}\text{U}$ ,  $^{236}\text{U}$ , and  $^{238}\text{U}$ .

## 2. Radioactive Decay

### 2.1. Decay mechanisms

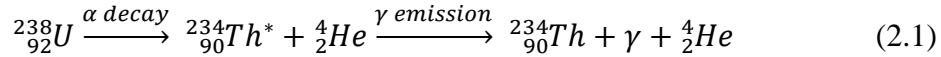
There are several mechanisms of radioactive decay (Figure 1); the most important ones to understand for U-Pb geochronology are alpha decay and beta decay. A radioactive parent isotope has an unstable nucleus, and over time it will decay to a daughter isotope.

Alpha decay: the parent atom emits an  $\alpha$  particle, which is a helium atom with mass 4 (2 protons and 2 neutrons, i.e.  $^4_2\text{He}$ ). The daughter atom has two fewer protons, and its atomic mass is decreased by four. After the  $\alpha$  particle is ejected, the daughter atom remains in an excited,

Type	Nuclear equation	Representation	Change in mass/atomic numbers
Alpha decay	$^A_Z\text{X} \rightarrow ^4_2\text{He} + ^{A-4}_{Z-2}\text{Y}$		A: decrease by 4 Z: decrease by 2
Beta decay	$^A_Z\text{X} \rightarrow ^0_{-1}\text{e} + ^A_{Z+1}\text{Y}$		A: unchanged Z: increase by 1
Gamma decay	$^A_Z\text{X} \rightarrow ^0_0\gamma + ^A_Z\text{Y}$		A: unchanged Z: unchanged
Positron emission	$^A_Z\text{X} \rightarrow ^0_{+1}\text{e} + ^A_{Z-1}\text{Y}$		A: unchanged Z: decrease by 1
Electron capture	$^A_Z\text{X} + ^0_{-1}\text{e} \rightarrow ^A_{Z-1}\text{Y} + \gamma$		A: unchanged Z: decrease by 1

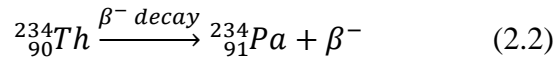
**Figure 1.** Modes of radioactive decay and their associated equations. X is the parent atom, Y is the daughter atom, A is the atomic mass, and Z is the atomic number (the number of protons in the nucleus).

unstable state. It then emits a  $\gamma$ -ray (photons with wavelength  $< 10^{-12}\text{m}$ ) and returns to ground state. For example,

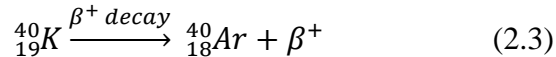


where \* denotes the excited (high-energy, unstable) state of the nucleus.

**Beta decay:** a process by which either a negatron ( $\beta^-$ ) or positron ( $\beta^+$ ) is emitted from the nucleus of the parent atom; the atomic mass of the daughter atom is the same as the parent, but the Z number is different. In  $\beta^-$  decay, a neutron is converted to a proton. For example,



In  $\beta^+$  decay, a proton is converted to a neutron. For example,



## 2.2. Radioactive Decay Constants and Half-Life:

Radioactive decay is not caused by external forces or events; rather it is an individually random, but statistically predictable process. The probability that a radioactive atom will decay is expressed by its **decay constant**,  $\lambda$ : the rate at which, on average, decays will occur per year. The **half-life**,  $t_{1/2}$ , is the length of time it takes for half of the parent isotope to have decayed to the daughter isotope:

$$t_{1/2} = \frac{\ln(2)}{\lambda} \quad (2.4)$$

$t_{1/2}$  is expressed in units of years (y);  $\lambda$  is expressed in units of atoms per atoms per year (i.e. probability of decay per year, or  $\text{y}^{-1}$ ). Figure 1 shows an example if you start with 24 atoms of a radioactive isotope with  $t_{1/2} = 5$  years.

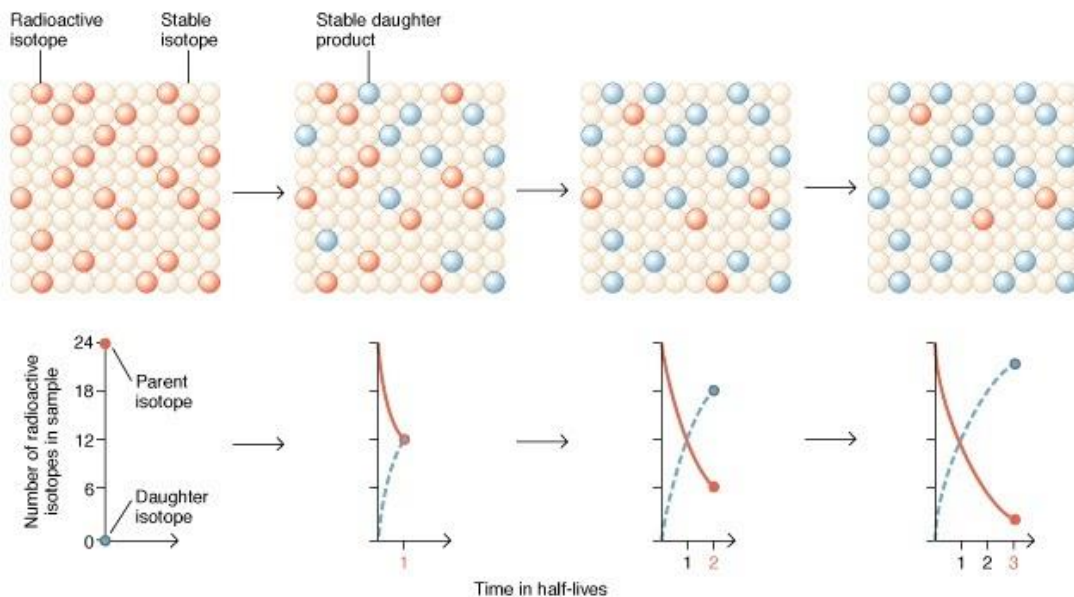


**Figure 2.** Schematic illustration of decay of radioactive parent isotope (orange) and accumulation of daughter isotope (blue) over the duration of three half-lives.

### 2.3. The Decay Equation

The quantity of a parent isotope over time is expressed with the differential equation:

$$\frac{dP}{dt} = -\lambda t \quad (2.5)$$

where  $P$  is the parent isotope,  $t$  is time (y), and  $\lambda$  is the decay constant ( $y^{-1}$ ). Integrating over time gives:

$$P = P_0 e^{-\lambda t} \quad (2.6)$$

where  $P_0$  is the initial quantity of parent isotope (at time  $t=0$ ), and  $P$  is the quantity at time  $t$ . Because the initial number of parent atoms  $P_0 = P + D^*$  ( $D^*$  = radiogenic daughter atoms), Eq. 2.6 becomes:

$$D^* = P(e^{\lambda t} - 1) \quad (2.7)$$

In most natural materials, however, there is some initial daughter isotope ( $D_0$ ) inherited when the material is formed. Total  $D = D_0 + D^*$ ; to account for *all* of the daughter isotope in the material, Eq. 2.7 becomes:

$$D = D_0 + P(e^{\lambda t} - 1) \quad (2.8)$$

The decay equation (Eq. 2.8) forms the basis for calculating radiometric ages in multiple isotopic systems. It can be solved for  $t$  assuming  $\lambda$  is known,  $D$  and  $P$  can be accurately measured in the sample, and  $D_0$  can be resolved. This reading focuses on ages calculated using the decay of uranium to lead.

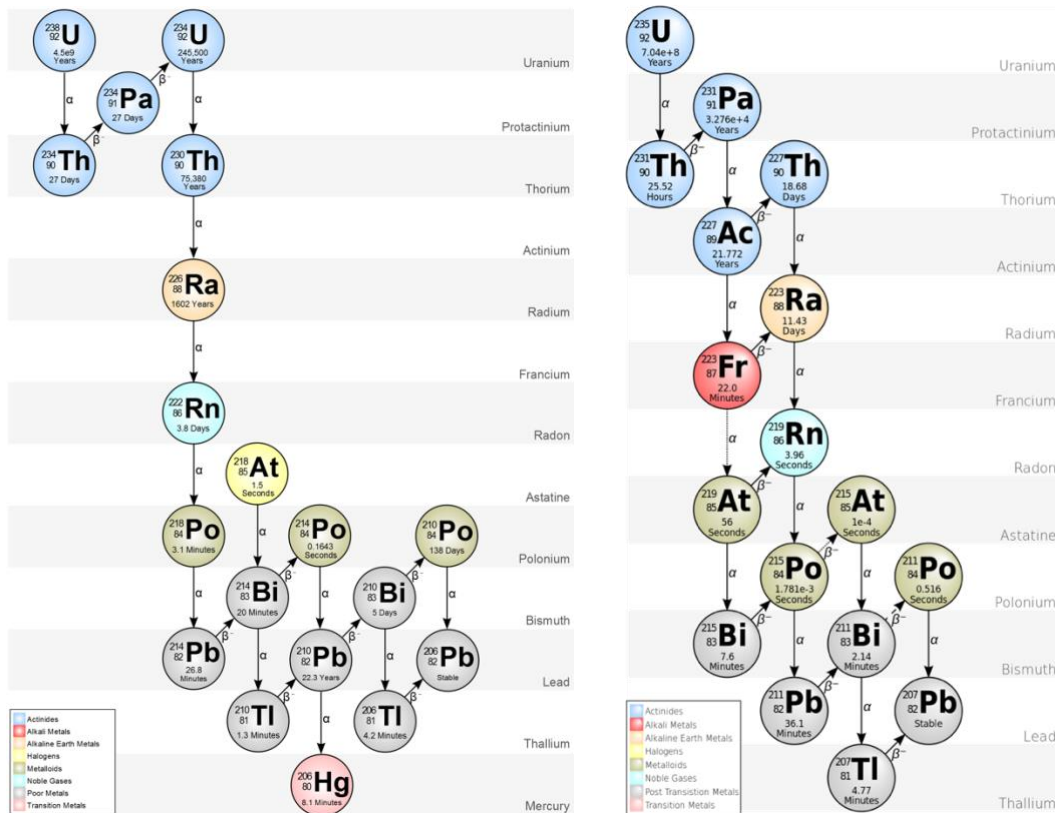


**Figure 3.** Decay chains of  $^{238}\text{U}$  (left) and  $^{235}\text{U}$  (right). Schematic axes represent changes in atomic number (up and down), and subtraction of neutrons (left to right).  $t_{1/2}$  are shown for each element.

### 3. U-Pb Geochronology

#### 3.1. U-Pb Decay Chains

All isotopes of uranium (U) are radioactive. The two most abundant isotopes of U are  $^{238}\text{U}$  and  $^{235}\text{U}$ . Both isotopes undergo a radioactive decay chain, which proceeds through multiple alpha and beta decays, producing intermediate daughter products, until the final stable daughter product is reached (Figure 3, Wikimedia Commons, 2020). The stable daughter product of  $^{238}\text{U}$  is  $^{206}\text{Pb}$ , and the stable daughter product of  $^{235}\text{U}$  is  $^{207}\text{Pb}$ . U-Pb radiometric dating only requires measurement of the original parent isotope (U) and the stable daughter product (Pb).

Parent	Daughter	$t_{1/2}$ (y)	$\lambda$ ( $\text{y}^{-1}$ )
$^{238}\text{U}$	$^{206}\text{Pb}$	$4.468 \times 10^9$	$1.55 \times 10^{-10}$
$^{235}\text{U}$	$^{207}\text{Pb}$	$7.04 \times 10^8$	$9.857 \times 10^{-10}$

#### 3.2. U-Pb Age Equations

The two U isotopes yield two decay equations:

$$^{206}\text{Pb} = ^{206}\text{Pb}_o + ^{238}\text{U}(e^{\lambda_{238}t} - 1) \quad (3.2a)$$

$$^{207}\text{Pb} = ^{207}\text{Pb}_o + ^{235}\text{U}(e^{\lambda_{235}t} - 1) \quad (3.2b)$$

where  $Pb_o$  is initial Pb in the sample (at time  $t = 0$ ), and  $\lambda_{238}$  and  $\lambda_{235}$  are the decay constants of  $^{238}\text{U}$  and  $^{235}\text{U}$ , respectively. If  $Pb_o$  is minimal, or can be calculated (see section 3.4), then the equations can be solved for  $t$ , i.e. the radiometric age of the sample. If the radiogenic elements in a sample have not been disturbed following crystallization, then the value of  $t$  calculated for both Eq. 3.2a and 3.2b should be the same. The U-Pb age of the sample is therefore said to be concordant. However, this is often not the case, either because of incorrect correction for  $Pb_o$  or because the system has experienced Pb-loss at some point between crystallization and today. These factors can be investigated using Concordia diagrams.

#### 3.3. Concordia Diagrams

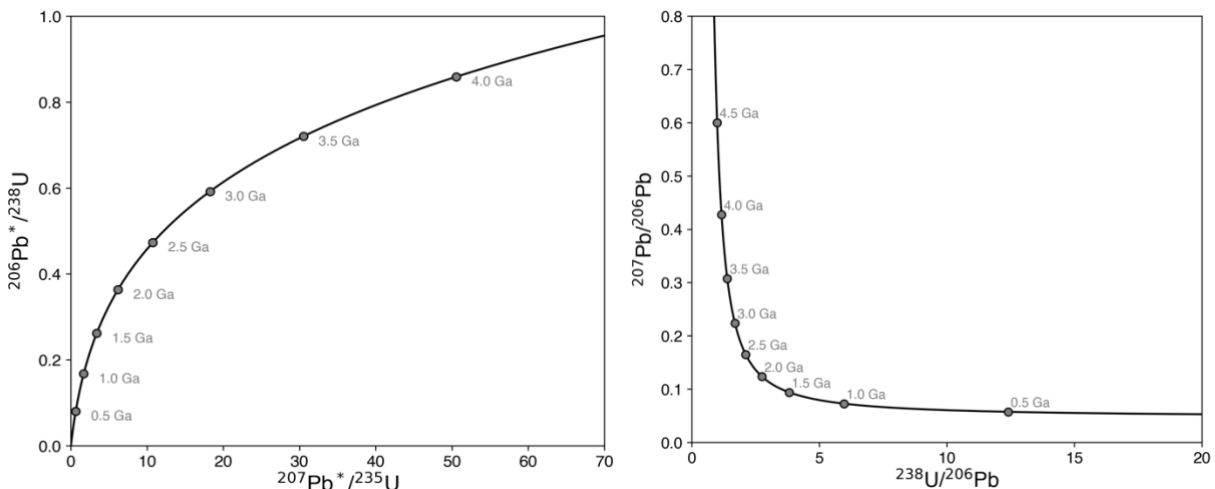


**Figure 4.** “Wetherill” Concordia diagram (left), and “Tera-Wasserburg” concordia diagram, right. The solid line shows the evolution of Pb/U ratios with time in a closed system. Data that fall along this line (“concordia”) are said to be concordant. \* indicates radiogenic Pb, i.e. does not include common Pb component ( $Pb_o$ ). Points on concordia show the ratios for ages in 0.5 billion-year intervals.

There are two versions of the “concordia” diagram: the more commonly used “Wetherill” concordia diagram, which plots  $^{207}\text{Pb}^*/^{235}\text{U}$  against  $^{206}\text{Pb}^*/^{238}\text{U}$ , as well as the Tera-Wasserburg concordia diagram, which plots  $^{238}\text{U}/^{206}\text{Pb}^*$  against  $^{207}\text{Pb}^*/^{206}\text{Pb}^*$  (Figure 2). When a mineral experiences *post-crystallization* disturbance of its radiogenic isotopes, its U-Pb ratios will no longer plot on concordia (Figure 5, modified from Allègre, 2008). The most common event is for the mineral to lose radiogenic Pb, which can result in partial or total resetting of U-Pb age. If the mineral is totally reset (i.e. it loses all radiogenic Pb accumulated since crystallization), it will again plot on concordia at the age when the Pb-loss occurred. More commonly, partial Pb-loss will cause data from the sample to fall on a linear array between crystallization age  $T_0$  (the older age) and  $T_1$  (the age when Pb-loss occurred). This linear array from Pb-loss can be used to constrain both the crystallization age of the mineral as well as the age when a metamorphic event caused to Pb-loss.

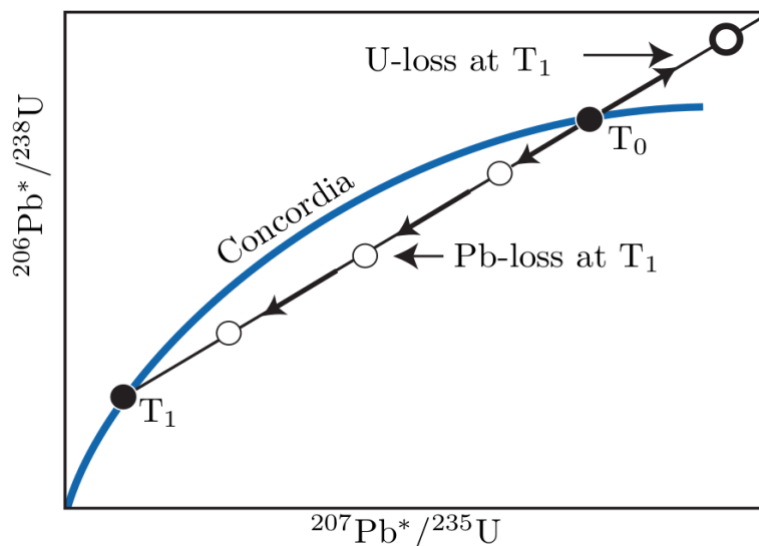


**Figure 5.** Schematic “Wetherill” Concordia diagram showing concordia (blue) as well as the ways U-loss and Pb-loss can affect whether data fall on concordia.  $T_0$  = crystallization age;  $T_1$  = age of Pb-loss or U-loss. Arrows show trajectory of Pb/U ratios in sample according to Pb-loss (from  $T_0$  to  $T_1$ ) or U-loss (from  $T_0$  away from  $T_1$ ). We can imagine the open circles between  $T_0$  and  $T_1$  as data from three minerals from a single sample measured in the laboratory. Because they did not all lose the same quantity of Pb, they form a linear array whose intercepts with concordia give crystallization age ( $T_0$ ) and metamorphic age ( $T_1$ ).

### 3.4. Laboratory analysis of U-Pb ages

There are several minerals that are commonly used as “geochronometers”: zircon ( $\text{ZrSiO}_4$ ), apatite ( $\text{Ca}_5(\text{PO}_4)_3(\text{F},\text{Cl},\text{OH})$ ), and titanite ( $\text{CaSiO}_5$ ) are all commonly used chronometers. They are useful because they incorporate trace amounts of U in their crystal lattice when they crystallize. Once these minerals have crystallized and cooled, the U is trapped inside the crystal. When it decays to Pb, that Pb is also trapped and preserved, as long as the mineral is not heated above the *closure temperature* of Pb – i.e. the temperature at which Pb can easily diffuse out of the crystal lattice. Only major heating events (over 400°C for apatite, 500°C for titanite, and 750°C for zircon) cause Pb loss.

Minerals measured for U-Pb in the laboratory are measured by mass spectrometer, either *in-situ* or by solution chemistry. For *in-situ* methods, the mineral is mounted, sectioned, and polished to

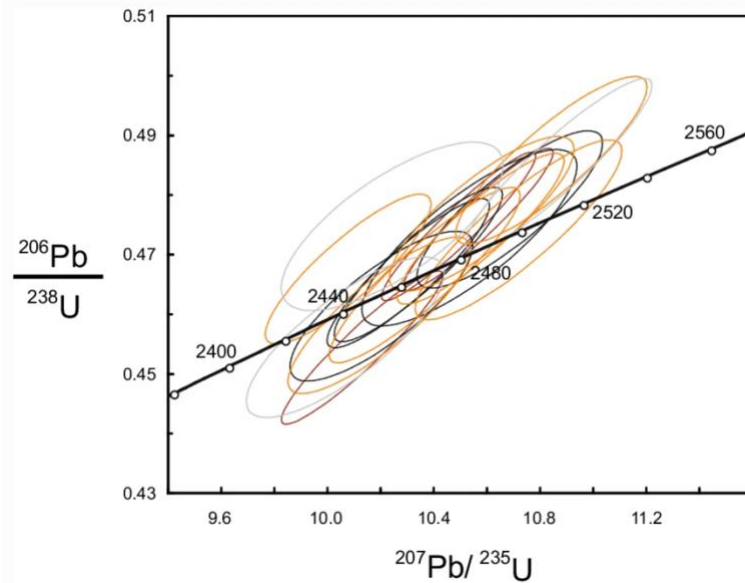


**Figure 6.** Example concordia diagram showing data from zircons in an Archean gneiss in Scotland. The black curve is concordia, the error ellipses derive from analytical error in  $^{206}\text{Pb}$ ,  $^{207}\text{Pb}$ , and  $^{238}\text{U}$  measurements, and calculated  $^{235}\text{U}$ .

reveal a cross-section of the grain. A laser or ion beam spot is pointed at the grain, where some of the material is ablated or sputtered from the surface. This material is ionized and travels through the mass spectrometer, where the U and Pb isotopes in the ionized material are measured. When measured by solution chemistry, the entire grain is dissolved, and its U and Pb components are chemically separated and fed into the mass spectrometer for U and Pb isotope measurement. For either method, the analyses are “standardized” by measuring U-Pb of a reference material with a well-known age, and correcting measurements based on the expected U-Pb isotopic composition of the reference material.

Zircon a very popular geochronometer because it not only incorporates U; it also incorporates less Pb during crystallization than apatite and titanite. The correction necessary for  $Pb_o$  (initial, non-radiogenic Pb) is therefore small. There are multiple methods to correct for  $Pb_o$  as well as common Pb (Pb that is introduced to the sample from outside sources, whether *in-situ* prior to sample collection or from laboratory contamination). The simplest way to correct for non-radiogenic Pb in a sample is to measure not only the parent and daughter products, but also the concentration of  $^{204}\text{Pb}$ , which is the only non-radiogenic isotope of Pb. The decay equations are then normalized by  $^{204}\text{Pb}$ , e.g.,

$$\frac{^{206}\text{Pb}}{^{204}\text{Pb}} = \left( \frac{^{206}\text{Pb}}{^{204}\text{Pb}} \right)_o + \frac{^{238}\text{U}}{^{204}\text{Pb}} (e^{\lambda_{238}t} - 1) \quad (3.3)$$

In zircon, inherited  $Pb_o$  is often insignificant, but can be calculated using various methods that deconvolve discordance in data and separate Pb-loss from inherited  $Pb_o$  (e.g., Andersen, 2002).

Additionally, because  $^{235}\text{U}$  is extremely low abundance relative to  $^{238}\text{U}$ ,  $^{235}\text{U}$  is not directly measured. Rather, it is “measured” by calculating its concentration from the amount of measured  $^{238}\text{U}$ . The modern ratio of  $^{238}\text{U}/^{235}\text{U}$  is known to be 137.8, so the concentration of  $^{235}\text{U}$  is calculated accordingly:

$$\frac{{}^{235}\text{U}}{{}^{204}\text{Pb}} = \frac{{}^{238}\text{U}}{{}^{204}\text{Pb}} * \frac{1}{137.8} \quad (3.4)$$

Because  ${}^{235}\text{U}$  is calculated using measured  ${}^{238}\text{U}$ , the errors in calculated  ${}^{207}\text{Pb}/{}^{235}\text{U}$  and  ${}^{206}\text{Pb}/{}^{238}\text{U}$  ages are correlated. Therefore, when U-Pb data are plotted on concordia diagrams, the uncertainty (error) in the data are plotted as ellipses (Figure 6, from Faithfull et al., 2018). Uncertainties in U-Pb ages are typically reported at the 95% confidence interval, 2-sigma ( $2\sigma$ ).

### 3.5. Detrital Zircon Geochronology

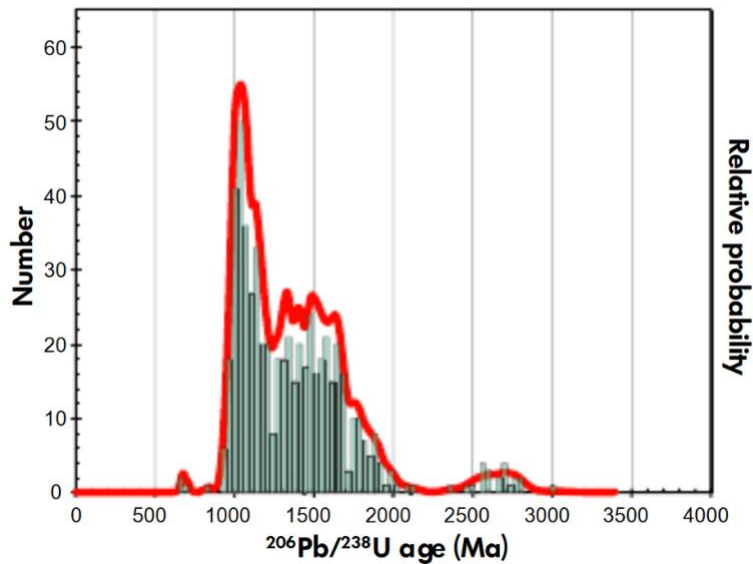


**Figure 7.** Probability density function (red) and histogram (green) of 1020 detrital zircons from a meta-sandstone in NW Ireland (modified from Chew et al., 2019). Note the small- $n$  populations at ca. 690 Ma and ca. 2700 Ma that may have gone undetected with fewer analyses.

As zircon is highly resistant to chemical and physical weathering, the zircon in sedimentary and metasedimentary rocks can be traced back to their unique protoliths by matching their ages (as well as other geochemical signatures). Data from detrital zircons can be used to investigate sediment origin, and determine proportions of different protoliths that contributed to the detrital zircons' host rock. Detrital zircon age data are often visualized as a histogram and/or probability density function, rather than on a concordia diagram, as the main interest of detrital studies is to capture populations of data that correspond to unique protolith units (e.g. Figure 7, modified from Chew et al., 2019).

Sample size may affect the accuracy of detrital zircon studies; datasets with few analyses may not identify small-number populations that are nevertheless of interest. Ideal detrital zircon datasets will include hundreds to thousands of analyses ( $n$ ) in order to fully capture the range of ages and compositions represented in the detrital population. For example, the oldest zircons on Earth are detrital zircons found in the Jack Hills Quartzite, Western Australia. Large- $n$  datasets (>100,000 grains) have allowed researchers to identify discrete populations of very old zircons, with the oldest individual grain dated to  $4371 \pm 12$  Ma ( $2\sigma$ ) (Figure 8, from Holden et al., 2009).

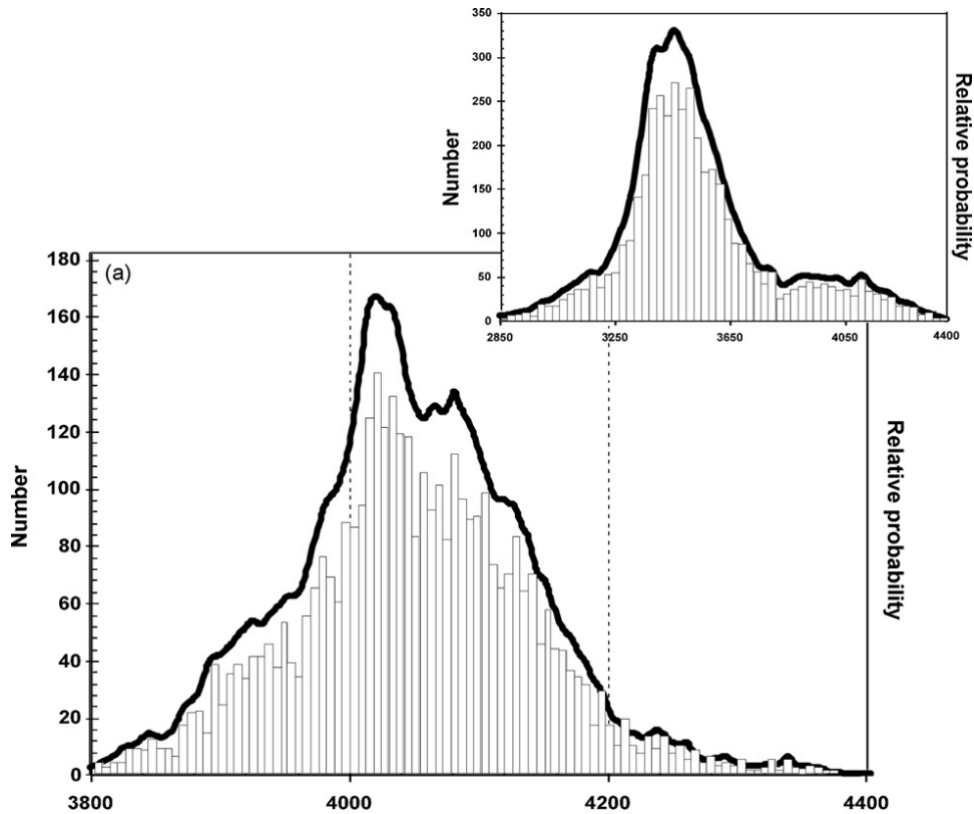


**Figure 8.** Histogram and probability density functions of concordant Jack Hills Zircons, extracted from a dataset of >100,000 grains analyzed. Hadean grains (>3800 Ma, (a)) represent a fraction of the population; the majority of grains are Eoarchean (2850 – 3800 Ma; inset). Of Hadean grains, the majority correspond to peaks at ca. 4050 and 4100 Ma, with smaller populations of younger and older grains. Modified from Holden et al., 2009.

Because Hadean grains make up only 5% of the population, large- $n$  studies were required to find these unique and important populations.

#### 4. U-Th-Pb<sub>Total</sub> Geochronology of Rare-Earth Phosphates

##### 4.1. Monazite and Xenotime U, Th, and Pb contents

Monazite (mnz) and Xenotime (xnt) are two additional accessory minerals useful for geochronology. Both are Rare-Earth-Element (REE) phosphates, with the general formula (REE)PO<sub>4</sub>. Mnz generally incorporates light REE (La to Eu; LREE), while xnt incorporates heavy REE (Gd to Lu; HREE). Through solid solution, mnz can incorporate significant amounts of Th and U; typical mnz contain ~6 wt. % ThO<sub>2</sub> and <1wt. % UO<sub>2</sub>. Xnt also incorporates actinides to a lesser degree, with a preference for U over Th. Additionally, both mnz and xnt incorporate <1 ppm Pb during crystallization (i.e. very low  $Pb_0$ ), and have a high closure temperature for Pb (>1000°C for mnz).

##### 4.2. U-Th-Pb<sub>Total</sub> Age Equations

Unlike traditional U-Th-Pb geochronology in which the radiogenic isotopes of U, Th, and Pb are individually quantified in order to solve the age equations (cf. § 3), U-Th-Pb<sub>Total</sub> uses the *total* concentration of all isotopes of U, Th, and Pb to solve the age equation. In order for this



calculation to yield a geologically useful radiometric age, there are several important assumptions built into this method:

1. Non-radiogenic Pb ( $Pb_o + Pb_c$ ) is negligible
2. Relative abundances of radiogenic parent and daughter isotopes are known
3. The radiogenic system has not been disturbed (i.e. no Pb-loss).

The method makes use of the decay equations for isotopes of U and Th, assuming no  $Pb_o$ :

$$^{206}Pb = ^{238}U(e^{\lambda_{238}t} - 1) \quad (4.1a)$$

$$^{207}Pb = ^{235}U(e^{\lambda_{235}t} - 1) \quad (4.1b)$$

$$^{208}Pb = ^{232}Th(e^{\lambda_{232}t} - 1) \quad (4.1c)$$

The total concentrations of U, Th, and Pb are measured and converted to ppm, such that:

$$Pb_T = [^{206}Pb] + [^{207}Pb] + [^{208}Pb] \quad (4.2a)$$

$$U_T = [^{238}U] + [^{235}U] \quad (4.2b)$$

$$Th_T = [^{232}Th] \quad (4.2c)^*$$

\*Note that isotopes of Th other than  $^{232}Th$  are short-lived intermediate daughter products of U decay; for this method  $Th_T$  is assumed to be entirely  $^{232}Th$ .

Because  $Pb_T$  is assumed to be entirely radiogenic, the right hand side of Eq. 4.2(a) can be substituted for the decay equations (4.1a-c):

$$Pb_T = 206 \frac{U_T * 0.9928}{238.04} (e^{\lambda_{238}t} - 1) + 207 \frac{U_T * 0.0072}{238.04} (e^{\lambda_{235}t} - 1) + 208 \frac{Th_T}{232} (e^{\lambda_{232}t} - 1) \quad (4.3)$$

where 238.04 is the average atomic weight of U, and 232, 206, 207, and 208 are the atomic weights of  $^{232}Th$ ,  $^{206}Pb$ ,  $^{207}Pb$ , and  $^{208}Pb$ , respectively.  $Pb_T$ ,  $U_T$ , and  $Th_T$  are the measured concentrations of Pb, U, and Th in ppm. Decay constants for  $^{238}U$ ,  $^{235}U$ , and  $^{232}Th$  are  $\lambda_{238} = 1.55 \times 10^{-10} \text{ y}^{-1}$ ,  $\lambda_{235} = 9.857 \times 10^{-10} \text{ y}^{-1}$ , and  $\lambda_{232} = 4.9475 \times 10^{-10} \text{ y}^{-1}$ , respectively. Eq. 4.3 is solved iteratively for  $t$  until the measured value  $Pb_T$  is matched.

#### 4.3. Laboratory Analysis of U-Th-Pb<sub>Total</sub> Ages

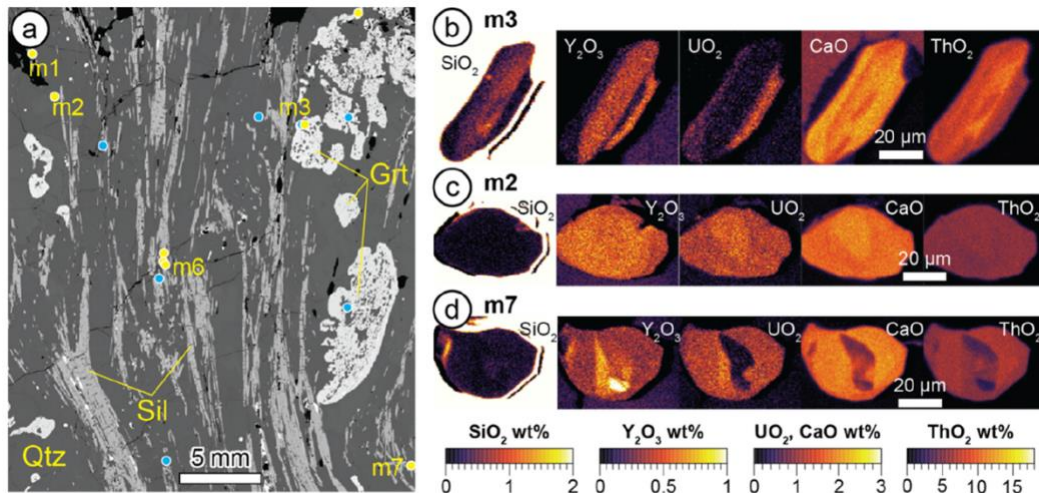


**Figure 9.** Example U-Th-Pb<sub>Total</sub> analysis of monazite in thin section: a) backscatter electron image from a full thin section WDS map with the identification of mnz grains (yellow dots) and zircon (blue circles). b-d) Quantitative element maps of SiO<sub>2</sub>, Y<sub>2</sub>O<sub>3</sub>, UO<sub>2</sub>, CaO and ThO<sub>2</sub> in the Mnz identified in a). (modified from Allaz et al., 2020)

Monazite and xenotime concentrations (in wt. % or ppm) of U, Th, and Pb are measured by electron microprobe (EPMA), either in thin section or in grain mounts of mineral separates. EPMA instruments have much lower sensitivity than mass spectrometers – detection limits are at best 50-100 ppm Pb, while mass spectrometers commonly can quantify ppb-level concentrations of Pb. Because Th and U are so abundant in these two minerals, they produce detectable quantities of Pb over relatively short periods of (geologic) time, and radiogenic Pb contributes >99% of measured Pb<sub>T</sub>.

EPMA electron beams can be focused to <0.5µm spot size, allowing for extremely high spatial resolution. This is particularly advantageous for analysis of monazite and xenotime, which are often ca. 10-100µm in diameter and thus difficult to target with other *in-situ* instruments. The high spatial resolution of EPMA and the high concentration of U and Th in monazite and xenotime enable quantitative mapping of U, Th, and Pb in individual grains. Quantitative mapping facilitates identification of chemical zonation and distinct age domains which may be associated with metamorphic or alteration events in the sample's history (Figure 9, modified from Allaz et al., 2020).

### Figure References

Allaz, J.M., Jercinovic, M.J., and Williams, M.L., 2020, U-Th-PbTOTAL dating of REE-phosphate by electron microprobe: Review and progress: IOP Conference Series: Materials Science and Engineering, v. 891, p. 012001, doi:10.1088/1757-899X/891/1/012001.

Allègre, C.J., 2008, Isotope Geology (C. Sutcliffe, Tran.): Cambridge, Cambridge University Press, doi:10.1017/CBO9780511809323.

Andersen, T., 2002, Correction of common lead in U–Pb analyses that do not report 204Pb: Chemical Geology, v. 192, p. 59–79, doi:10.1016/S0009-2541(02)00195-X.

Chew, D., Drost, K., and Petrus, J.A., 2019, Ultrafast, > 50 Hz LA-ICP-MS Spot Analysis Applied to U–Pb Dating of Zircon and other U-Bearing Minerals: Geostandards and Geoanalytical Research, v. 43, p. 39–60, doi:https://doi.org/10.1111/ggr.12257.

Decay chain, 2020, Wikipedia, [https://en.wikipedia.org/w/index.php?title=Decay\\_chain&oldid=995002103](https://en.wikipedia.org/w/index.php?title=Decay_chain&oldid=995002103) (accessed February 2021).

Faithfull, J.W., Dempster, T.J., MacDonald, J.M., Reilly, M., and EIMF, 2018, Metasomatism and the crystallization of zircon megacrysts in Archaean peridotites from the Lewisian complex, NW Scotland: Contributions to Mineralogy and Petrology, v. 173, p. 99, doi:10.1007/s00410-018-1527-5.

Holden, P., Lanc, P., Ireland, T.R., Harrison, T.M., Foster, J.J., and Bruce, Z., 2009, Mass-spectrometric mining of Hadean zircons by automated SHRIMP multi-collector and single-collector U/Pb zircon age dating: The first 100,000 grains: International Journal of Mass Spectrometry, v. 286, p. 53–63, doi:10.1016/j.ijms.2009.06.007.